

New Insights on the Compatibility of Nitrocellulose with Aniline-Based Compounds

Djalal Trache,^{*,[a]} Ahmed Fouzi Tarchoun,^{*,[a]} Salim Chelouche,^[a] and Kamel Khimeche^[a]

Abstract: In this paper, the compatibility of nitrocellulose (NC) with some aniline-based stabilizers was studied in order to detect any interaction between these materials. Both thermal techniques [differential scanning calorimetry (DSC) and vacuum stability test (VST)], and supplementary non-thermal techniques [Fourier transform infrared spectroscopy (FTIR), X-ray diffraction (XRD) and densimetry] were used. The thermal and non-thermal measurements showed

that NC was highly compatible with N-(2-methoxyethyl)-p-nitroaniline (MENA) and diphenylamine (DPA), while a degree of incompatibility is indicated for N-(2-acetoxymethyl)-p-nitroaniline (ANA). The compatibility of the different mixtures was further probed by the kinetic investigation, and the activation energy and the pre-exponential factors were computed. A detailed discussion and comparison of the compatibility results from all the methods are made.

Keywords: characterization · compatibility · kinetics · nitrate ester · stabilizer

1 Introduction


The compatibility of energetic materials with various ingredients such as stabilizers, catalysts, plasticizers, oxidizers, metal fuel, etc. is a crucial safety aspect related to their production, use and storage that should be thoroughly investigated at an early stage of the development of formulations. For practical reasons, materials are considered compatible if during and after a specific storage period the function and safety of the components are still acceptable [1].

Nitrate esters, one of the main classes of energetic materials, such as NC, nitroglycerine (NG), triethylene glycol dinitrate (EGDN), pentaerythritol tetranitrate (PETN) have been extensively used in various military and civilian applications for several years [2, 3]. Although a slow decomposition can occur even under normal conditions of temperature, pressure, and moisture, NC remains the most important nitrate ester that is widely utilized in gunpowders and solid propellant formulations [4–6]. Because of its chemical instability, such energetic component should contain some stabilizing agent to avoid a number of degradation phenomena that can lead to autocatalytic decomposition, self-heating as well as cook-off safety hazards, and consequently negatively affect both in-service time and reliability of the formulations [7–9]. The common stabilizers for nitrate esters-based energetic materials belong to aniline-based compounds such as diphenylamine (DPA), 2-nitrodiphenylamine (2-NDPA) and p-nitro-N-ethylaniline, (N-(2-methoxyethyl)-p-nitroaniline (MENA), N,N'-diethyl-N,N'-diphenylurea (C1, EC, ethyl centralite), N,N'-dimethyl-N,N'-diphenylurea (C2, MC, methyl centralite) and N-methyl N,N'-diphenylurea (AK-II) [10,11]. These additives act by removing nitrogen oxides formed during nitrate esters decom-

position. A detailed mechanism of nitrate esters degradation and stabilization process can be found in our recent reviews [12,13].

Excellent research works all over the world have focused on the synthesis of new aniline-based stabilizers [14,15], the understanding of the interactions occurred between them [16–18], and the evaluation of the stability and performance of related energetic formulations [2,7, 8,13,14], but without sufficiently addressing an exhaustive investigation about the compatibility issues for such combinations. Consequently, a number of stabilizers did not satisfy the development of nitrate-ester based energetic materials. Although DPA, considered as the first stabilizer introduced in 1889 by Alfred Nobel, is currently used for the industrial production of single base propellants, it has several disadvantages. In addition to its toxicity and environmental impact, it presents some compatibility issues with nitroglycerine and cannot be used for double base propellant formulations, because of its high basicity. On the other hand, P-methyl-N-nitroaniline (MNA) and N-ethyl-p-nitroaniline (ENA) have been proved to be quite effective stabilizers in propellants, but they easily crystallize because of their bad compatibility with NG and NC, which limited their application in solid propellant formulations. MENA and ANA, however, were previously reported as efficient stabilizers for composite double base propellants containing both nitro-

[a] D. Trache, A. F. Tarchoun, S. Chelouche, K. Khimeche
UER Procédés Energétiques, Ecole Militaire Polytechnique
BP 17, Bordj El-Bahri, 16046, Algiers, Algeria
*e-mail: djalaltrache@gmail.com
tarchounfouzi@gmail.com

 Supporting information for this article is available on the WWW under <https://doi.org/10.1002/prep.201800269>

cellulose and nitroglycerine in addition to other ingredients, but their evaluation as stabilizing agent for nitrocellulose in single base propellant to substitute DPA was not yet addressed, and no report highlighted the eventual issues of these stabilizers with pure nitrocellulose. Indeed, compatibility is a key parameter that has to be properly assessed prior to the formulation stage.

The compatibility of energetic materials, mainly explosive mixtures with inert/energetic ingredients such as explosives, binders, and plasticizers has been extensively investigated. However, compatibility studies dealing with aniline-based compounds and nitrate esters are very scarce. It is commonly considered obvious to use such stabilizers taking into account their stabilizing efficiency, without addressing any question about the existence of compatibility issues.

This crucial property was studied by several authors using various testing and analytical methods such as DSC, thermogravimetry, microcalorimetry, and VST [19–22]. Recently, FITR and XRD have been employed as efficient and complementary tools to evaluate physical characteristics or interactions between energetic components and to analyze their compatibility [23,24]. Standards and standardization of test methodologies for the compatibility assessment of energetic materials have been reported [25]. Furthermore, kinetics is a crucial approach used to investigate the compatibility of energetic materials, where the main purpose is to determine reaction mechanism and the parameters of the Arrhenius equation [26,27].

Therefore, the present study explored various thermal and non-thermal techniques as well as kinetics for the analysis of the compatibility between NC and some aniline-based stabilizers, which were commonly used in solid propellant formulations. A detailed discussion of the experimental results will be presented as well, in order to get a better insight into the selection of a suitable stabilizer.

2 Experimental Section

2.1 Materials

Conventional nitrocellulose (NC), synthesized in a laboratory using Alfa grass fibers (one of the most abundant sources of cellulose in Algeria) as described previously [6], was used for the elaboration of (NC/stabilizer) films. The physicochemical properties of the nitrated cellulose used are given elsewhere [6].

Some of the stabilizers MENA and ANA were synthesized and purified following the method indicated in the work of Gibson [28]. Their purity was checked by DSC, UV-visible, and high-performance liquid chromatography instrument, and evaluated to be greater than 98%. DPA was provided by Sigma-Aldrich with purities greater than 99%. It was used without further purification. The chemical structures of the investigated stabilizers are given in Figure 1.

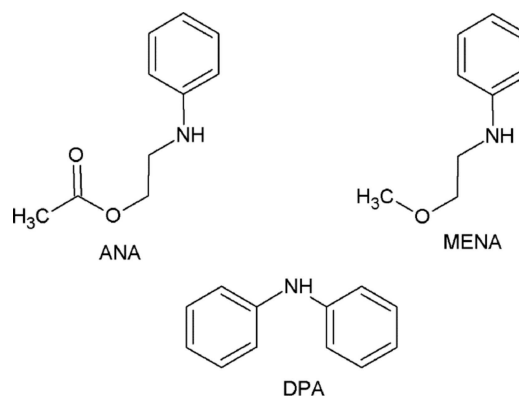


Figure 1. Chemical structure formulas of the stabilizers: ANA, N-(2-acetoxyethyl)-p-nitroaniline; MENA, N-(2-methoxyethyl)-p-nitroaniline; DPA, diphenylamine.

2.2 Preparation of (NC/Stabilizer) Membranes

The pure components were initially dried in an oven at 50 °C for 48 h, and then each mixture system (NC + DPA, NC + MENA, and NC + ANA) was prepared by a dissolving process in acetone using 97.0 wt.% NC and 3.0 wt.% stabilizer with continuous stirring until complete dissolution. After that, each sample is poured into glass Petri dishes for drying at room temperature to produce homogenous membranes. These films were ground/cut, put in vials and stored in a desiccator. This methodology ensured that the only difference between the samples produced was the type of stabilizer added. The preparation of various films is graphically presented in Figure S1 in the ESI.

2.3 Apparatus and Methods

Differential scanning calorimetry (DSC) was applied to study the thermal decomposition under linear heating. DSC curves were obtained using a NETZCH DSC type 204F1 phoenix analyzer, previously calibrated with high purity indium. The samples to be examined were taken and sealed in an aluminum crucible in portions of 1–2 mg. All experiments were performed in a nitrogen flow atmosphere (20 cm³ min⁻¹) from 50 °C to 270 °C at a heating rate of 10 °C min⁻¹. The results represent an average of three measurements.

The vacuum stability tester (VST, type STABIL, OZM research), which measured the amount of gas evolved from the thermal decomposition of a sample under certain vacuum and temperature conditions, was used to evaluate the compatibility of the different investigated mixtures. A typical VST instrument consists of a computer-controlled unit, heating block, sensitive pressure transducers, and a data acquisition and processing unit. It is capable to test multiple samples (up to 10) from a single control unit. The detailed components are outlined elsewhere [29]. 2.000 ± 0.001 g of

each sample was placed in the bottom of glass test tube. The tubes were evacuated below 0.2 kPa, sealed and placed in the thermostatic block. The samples were heated isothermally for 48 h at different temperatures 90, 100 and 110 °C, with the data-acquisition rate of 1 min⁻¹. The obtained results represented an average of three measurements.

Bergmann-Junk (BJ) test is one of the main quantitative tests for the evaluation of the stability of nitrate ester-based propellants. For our experiments, 0.5 g of each sample was heated at 132 °C for 5 hours. The evolved nitrogen oxides (NO) were entrapped in a secondary tube containing 50 ml of H₂O₂ (3.0 wt.%). The evolved NO gases were quantitatively determined by titration using NaOH (0.01 N) solution.

Fourier transforms infrared spectroscopy (FTIR) analysis was performed using a Shimadzu spectrometer 8400 S. The dried samples were embedded in potassium bromide (KBr) pellets. The spectra were collected in the transmittance band mode with a resolution of 4 cm⁻¹, in the range of 4000–400 cm⁻¹. 32 scans were co-added in order to achieve an acceptable signal to noise ratio. Compatibility was judged by comparing the FTIR spectrum of pure NC with those of the different mixtures.

X-ray diffraction (XRD) patterns were obtained using a PANalytical X'pert PRO Multi-Purpose diffractometer with Cu K α radiation at a generator voltage of 45 kV with a generator current of 40 mA. The scan rates were in the 2 θ range from 5° to 50° with a step size of 0.017°/2 θ and a count time of 50.1650 s at each step. The crystallinity index of samples was calculated from the ratio of the total area of the crystalline peaks to the total area of coherent scatter above the background using the following equation:

$$ka = \frac{\sum Scr}{\sum Scr + \sum Sam} \quad (1)$$

Where ka the relative degree of crystallinity, Scr is the peak area for the crystalline part, and Sam is the peak area for the amorphous part.

The compatibility was assessed by comparing the X-ray diffractograms and the degree of crystallinity of pure NC with those of the various mixtures.

The densities of all samples were also measured using an electronic densimeter, type Accupyc 1340 II Pycnometer. The densimeter instrument consists of a computer control unit, an electric balance, a bottle of helium gas and a densimeter type gas pycnometer Accupyc II 1340. Three measurements were performed for each sample. The percentage gap between actual and maximum theoretical density is defined by [30]:

$$\Delta\rho_p = \frac{\rho_{exp} - \rho_{th}}{\rho_{th}} \times 100 \% \quad (2)$$

The compatibility was evaluated by comparing the density value of pure NC with those obtained for different (NC + stabilizers) mixtures.

2.4 Kinetic Analysis

The compatibility determination using VST measurements can be performed on the basis of the analysis of the kinetic parameters of the decomposition process. For this purpose, isothermal measurements are performed at three different temperatures (90 °C, 100 °C and 110 °C) over 48 h.

Complete kinetic description of thermally stimulated reactions in solids could be reached by the determination of the kinetic triplet, including the activation energy (E_a), the frequency factor (A) and the reaction model $g(\alpha)$. Such analysis can be conducted in two main ways: isoconversional (model-free) and model-fitting methods [31]. Each of these methods can be used for isothermal and nonisothermal processes. In the present work, the kinetic parameters have been determined under isothermal conditions, where the kinetic model-fitting method in its integral form was performed based on the following equation [26, 29]:

$$g(\alpha) = K(T) t \quad (3)$$

Where α is the extent of conversion ($0 \leq \alpha \leq 1$), t is the time, T is the absolute temperature, $K(T)$ is the temperature dependent rate constant and $g(\alpha)$ is the integrated form of the reaction model that represents the reaction mechanism. The value of α is experimentally derived from VST data using the following equation:

$$\alpha = \frac{P - P_0}{P_{max} - P_0} \quad (4)$$

Where P_{max} is the maximum pressure at the end of the reaction, p is the pressure at any time, and p_0 is the initial pressure.

The isothermal kinetics processing approach employed 41 types of reaction models $G(\alpha)$ to determine the kinetic parameters [32]. The substitution of these reaction models into Eq. (3) allowed the determination of the corresponding rate constant, which is obtained from the slope of the plot of $G(\alpha)$ vs. t . The most proper form of $G(\alpha)$ is selected according to the better correlation coefficient (r^2) [19]. All the calculations mentioned above were run by a program compiled by means of MATLAB software [32].

The isokinetic theory has been widely applied to investigate physical and chemical phenomena [33]. The isokinetic temperature (T_{iso}) is the actual temperature at which rates of all members of a series of related reactions are equal, which is often close to, or within, the temperature interval of the measured kinetic data. T_{iso} originates from the compensation effect, which manifests in a linear correlation between E_a and the Neperian algorithm of the Ar-

Arrhenius pre-exponential factor A (also called Cremer-Constable relation) [34].

$$\ln(A_i) = a + bE_{ai} \quad (5)$$

where a and b are constants. With the Arrhenius equation, we obtain.

$$\ln(A_i) = \ln(K_i) + \frac{1}{RT} E_{ai} \quad (6)$$

The corresponding Arrhenius lines have a common point intersection, which is the isokinetic point, where $a = \ln(k_{iso})$ and $1/(b \cdot R) = T_{iso}$.

3 Results and Discussion

3.1 DSC Analysis

The DSC curves for all samples (NC, NC/DPA, NC/MENA and NC/ANA) are presented in Figure 2. The criteria used to evaluate the compatibility between NC and the different stabilizers are inspired from the NATO standardization agreement STANAG 4147, which stipulates that acceptable compatibility is confirmed if there is less than 4 °C depression in the temperature of the peak exotherm. Furthermore, this standard outlined that the appearance/disappearance of new/old peaks means that the mixture is incompatible [25, 35].

It must be noted that while the STANAG 4147 document calls for DSC analyses to occur at 2 °C min⁻¹, the results reported here are from analyses at 10 °C min⁻¹. A series of runs at both scan rates was performed and analysis of the data showed no discernable difference in the results. Therefore, 10 °C min⁻¹ are chosen to minimize analysis time. The DSC profile curve of the pure NC revealed a single decomposition event with an exothermic peak temperature of

206.57 °C. Moreover, there exists only a single decomposition event even for NC/DPA and NC/MENA mixtures. For these two mixtures, the resulting peak temperatures are 2.25 °C and 0.83 °C higher than that pure NC, respectively. Therefore, DPA and MENA are both compatible with pure NC according to the STANAG 4147 criterion. However, the DSC curve of NC/ANA consists of two decomposition events at lower temperatures, where the first decomposition peak is 10.83 °C lower than that of the pure NC. Thus ANA is incompatible with NC according to STANAG 4147, despite its ability to fix nitrous oxide which is generated from the NC degradation [12].

3.2 VST and BJ Analyses

The criterion for compatibility by the VST in STANAG 4147 is based on a maximum variation of 5 ml/5 g additional evolved gas for the tested mixture of compounds against that of the pure energetic material. The results of VST provided the volume of liberated gas (Figure 3(a)) and the evolved gas pressure (Figure 3(b)) at 100 °C for 48 hours by pure NC, NC/DPA, NC/MENA, and NC/ANA mixtures. It can be seen from Figure 3 that the VST values of the NC/DPA and NC/MENA are lower than the VST values of pure NC. Therefore, DPA and MENA are compatible with NC according to the STANAG 4147. However, the mixture NC/ANA displays an intense increase in the volume of gas liberated (7.32 ml g⁻¹) as well as the evolved pressure indicating the presence of incompatibility. This behavior could be probably due to the interaction between NC/ANA in solid phase as well as with the gaseous products; however, the definite mechanism needs further investigation.

The results obtained by BJ test show some agreement with those obtained by VST test (in terms of the volume of gases released by each sample). However, the values obtained by VST are relatively larger compared to those obtained by BJ test, which makes sense, because the VST measures the volume of all gases released (CO, CO₂, N₂, NO_x), while the BJ test measures only the volume of the evolved nitric oxide (NO).

As can be seen in Figure 3(a), the nitrocellulose samples stabilized with DPA and MENA have a lower release of nitric oxide than pure NC, which confirms the stabilizing effect of DPA and MENA. In contrast, the nitrocellulose stabilized with ANA presents a higher NO_x released than that of the pure NC, which indicates and confirms the bad stabilizing effect of this stabilizer, and its incompatibility with NC.

3.3 FTIR and XRD Analyses

FTIR spectroscopy was used as a non-thermal analytical technique for the detection of eventual changes induced by an incompatibility in the NC/stabilizer mixtures. The FTIR spectra of the tested samples are shown in Figure 4 (a) and

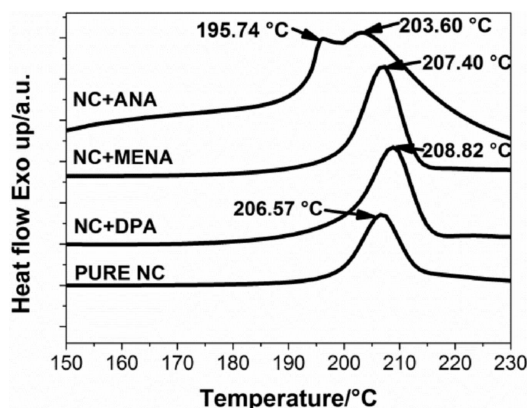


Figure 2. DSC curves of pure NC and its mixture systems (NC/stabilizer) at a heating rate of 10 °C min⁻¹.

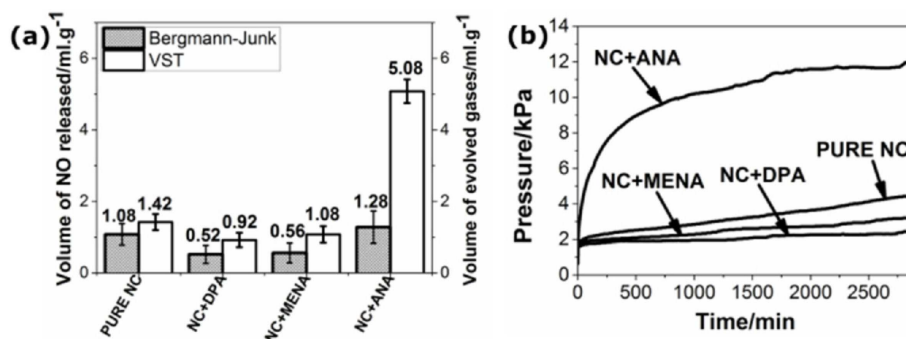


Figure 3. (a) Comparison between the volume of nitrogen oxide determined by BJ test and the volume of gases determined by VST (at 100 °C for 48 h), released by pure NC and its mixtures; (b) The gas-evolved pressure of the pure NC and its mixtures (NC/stabilizer) at 100 °C for 48 hours.

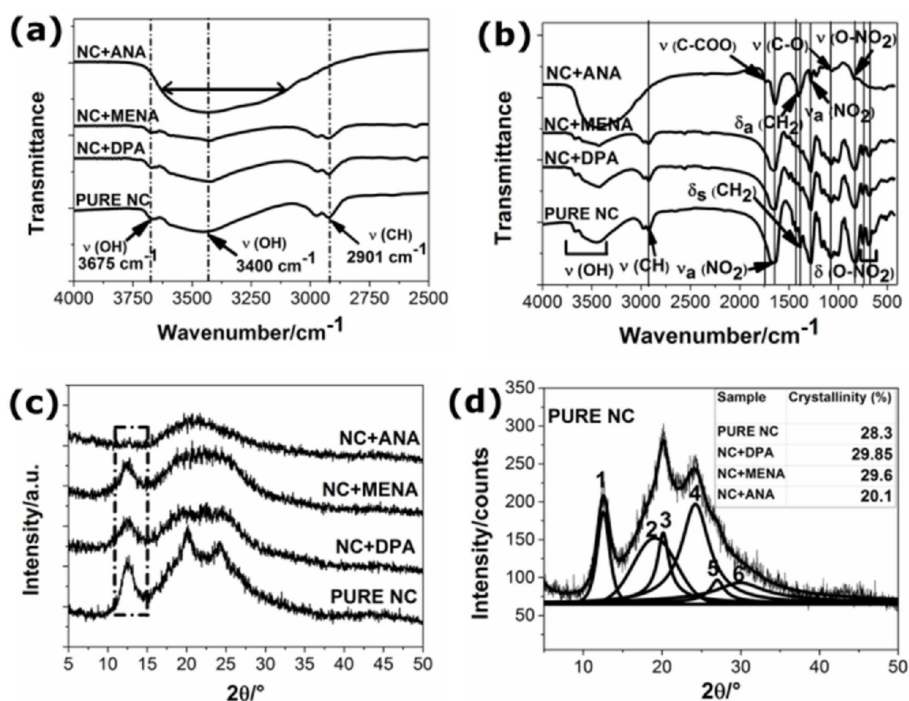


Figure 4. (a) FTIR spectra of pure NC and its mixtures in the spectral range of 4000–2500 cm⁻¹; (b) FTIR spectra of pure NC and its mixtures in the spectral range of 4000–400 cm⁻¹; (c) X-ray diffractogram of pure NC and its mixtures; (d) Peak separation of X-ray diffractometry profile of pure NC.

(b). With regard to the FTIR spectra of NC/DPA and NC/MENA, all the characteristic bands of the pure NC can be observed, without the absence, shift or broadening of the characteristic band, or the formation of new peaks. This result suggests the absence of chemical interactions between NC and the corresponding stabilizer.

As seen in Figure 4 (a) and (b) for the FTIR spectra of NC/ANA mixture, several changes are observed, the disappearance of the band at 3675 cm⁻¹ is attributed to the elongation vibration of the free OH group, and the enlargement of the band at 3400 cm⁻¹ is attributed to the elongation vibration of the linked OH group. The disappearance of

the band at 2901 cm⁻¹ is assigned to the elongation of the C–H stretching vibration, the appearance of the band at 1738 cm⁻¹ concerned the elongation vibration of the acetoxy (C–COO) group. The disappearance of the band at 1428 cm⁻¹ is attributed to the asymmetric CH₂ bending vibration, and the disappearance of the band at 690 cm⁻¹ is assigned to the deformation vibration of the O–NO₂ group. These results clearly provide evidence for possible chemical interactions in the mixture.

XRD has been used to investigate possible chemical interactions and changes in crystallinity between NC and different stabilizers, which is a direct measure for revealing

Table 1. Densities and Arrhenius parameters for isothermal decomposition of NC and its mixtures.

Samples	Arrhenius parameters			r^2	E_a -adj (kJ mol ⁻¹)	Ln(A)-adj (s ⁻¹)	Densities		
	E_a (kJ mol ⁻¹)	Ln(A) (s ⁻¹)	$g(\alpha)$				ρ_{exp} (g cm ⁻³)	ρ_{th} (g cm ⁻³)	$\Delta\rho_p$ (%)
Pure NC	139 ± 2	30 ± 1	1-(1- α) ³	0.9786	139.87 ± 0.23	30.93 ± 0.04	1.7092	–	–
NC/DPA	182 ± 2	43 ± 2	1-(1- α) ³	0.9874	182.08 ± 0.23	44.67 ± 0.04	1.7122	1.6877	1.45
NC/MENA	192 ± 2	47 ± 1	1-(1- α) ⁴	0.9732	192.81 ± 0.23	48.25 ± 0.04	1.6985	1.6925	0.35
NC/ANA	85 ± 2	13 ± 1	1-(1- α) ⁴	0.9767	85.65 ± 0.23	13.24 ± 0.06	1.6406	1.6987	3.42

unique diffraction patterns that contain the fingerprints of individual components. Such technique could be used for compatibility assessment of energetic materials, but it has limited detection level compared to the thermal analysis methods.

As can be seen from Figure 4 (c), all the characteristics peaks of the pure NC are observed in the diffractograms of the mixtures NC/DPA and NC/MENA, suggesting that there are no interactions between NC and the corresponding stabilizers.

Unlike NC/DPA and NC/MENA mixtures, the experimental XRD pattern for NC/ANA shows the absence of the peak at 12.5°, thus chemical interactions can be suspected for the NC/ANA mixture. The peak at 12.5° was considered by several authors as a superposing double peak, assigned to one part of the crystalline domain of NC [6,36,37], whereas the halo appearing between 15–35° is attributed to the less ordered region of the cellulosic chains. As considered by Herrmann et al. [37], this latter is composed of crystalline and amorphous domains. They stipulated that the mathematical treatment of the XRD data of NC by means of the deconvolution with Pearson VII function would give fruitful information allowing the determination of the crystallinity. These authors have employed this procedure to determine the crystallinity of various nitrocelluloses and have investigated the effect of crystallinity of NC on the viscosity and fineness. These authors demonstrated that this procedure provides interesting and coherent results of crystallinity. This methodology was also adopted in our recent work, where we have demonstrated an increase of the crystallinity of microcrystalline nitrocellulose with respect to the ordinary one. Figure 4 (d) depicts the peak separations of X-ray diffraction profile of pure NC, using Pearson VII function. This method is widely used and proven in the literature [6,37]. The calculated crystallinity data show that the crystallinity indexes of NC/DPA and NC/MENA mixtures are close to that of pure NC, whereas that of NC/ANA mixture is lower, which indicates and confirms the incompatibility between NC and ANA.

3.4 Density Measurements

Density measurements were used as a supplementary method for the investigation of compatibility in the NC/stabilizer mixtures. The obtained density values of NC and its

mixtures are listed in Table 1. The densities of NC/DPA and NC/MENA mixtures are close to that of the pure NC. In the case of the NC/ANA mixture, however, there is a decrease in the density, which is caused by a certain incompatibility, a conclusion that agreed with other methods. Furthermore, the experimental densities of samples almost agreed well with their theoretical values. The percentage gap calculated does not exceed 2% for DPA and MENA; consequently, it is negligible, which indicates that the samples homogenization has been successfully completed, whereas a slight increase beyond the expected 3% was found for ANA.

3.5 Calculation of Isothermal Reaction Kinetics of VST Data by Model Fitting Methods

The VST curves for all involved materials, shown in Figure 5, basically obey a parabolic trend with heating time, except for NC/MENA mixture where the pressure tended to increase rapidly after 1700 min of heating at 110 °C. However, this increase remained reasonable compared to that recorded for NC/ANA mixture, where the pressure increase was much more pronounced. The released gas pressure for all the studied samples at various isothermal temperatures (90 °C, 100 °C and 110 °C) was plotted versus time. At the beginning, the pressure increases rapidly and the pressure growth rates are conform to the increasing isothermal temperature, confirming the effect of temperature on the acceleration of thermal homolysis process of NC based formulations [12]. It is observed that the decomposition accompanied by gas formation proceeds slowly and smoothly in a long duration at 90 and 100 °C.

With regard to the effect of stabilizers on the evolution of the pressure as a function of time, it can be seen from Figures 5 and Figure 6 that the NC/DPA and NC/MENA mixtures have a moderate pressure evolution compared to that of the pure NC. Unlike the NC/ANA mixture which shows an intense increase in pressure compared to the pure NC. These findings are valid for all three test temperatures (90 °C, 100 °C and 110 °C), except for the NC/MENA mixture analyzed at 110 °C (Figure 6c) which exhibited greater gas formation and pressure than pure NC after the first 2000 minutes.

The isothermal kinetics are commonly considered as effective and complementary tools to confirm results obtained by thermal and non-thermal methods. In our case,

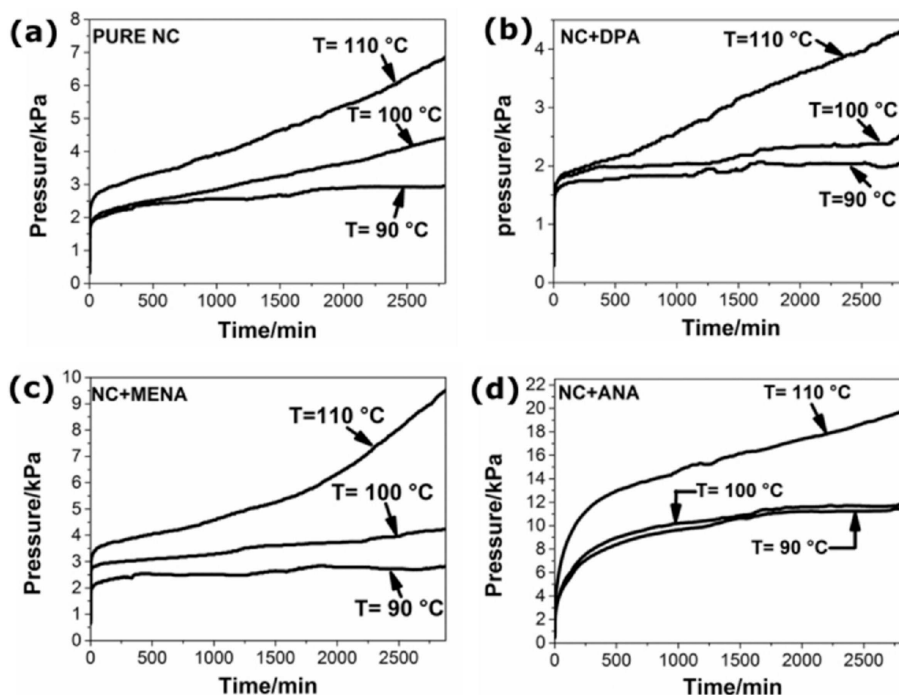


Figure 5. Gas-evolved pressure/*p* vs. time/*t* at different temperature; (a) Pure NC; (b) NC/DPA; (c) NC/MENA, (d) NC/ANA.

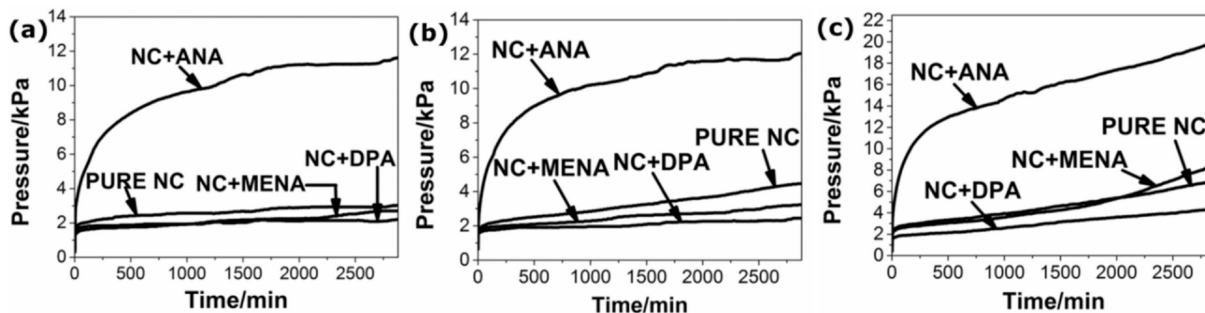


Figure 6. Effect of the type of stabilizer on the evolution of the gas pressure released at (a) 90 °C; (b) 100 °C; (c) 110 °C.

the best fitting kinetic parameters obtained by isothermal decomposition of pure NC, NC/DPA, NC/MENA, and NC/ANA are reported in Table 1. The correlation coefficient (r^2) is used as a parameter for choosing the best model fitting. The quality of data description with the chosen models is graphically shown in Figure 7.

It is worthy to note that E_a signifies the minimum energy level that the colliding molecules must possess in order to undergo a given chemical reaction [38].

The activation energy of pure NC obtained by VST is in agreement with the previous reports [6]. The E_a values of NC/DPA and NC/MENA mixtures are higher than that of pure NC, whereas the E_a obtained for the NC/ANA mixture is lower.

The E_a and $\ln(A)$ obtained for NC, NC/DPA, and NC/MENA, respectively, are both evidently higher than those of

NC/ANA. A proper kinetic interpretation should include the compensation effect, which is usually used to explain whether the variation on effective activation energy values have physical meaning or they are caused by either the propagation of experimental errors or the intrinsic mathematical consequences of the physical description of the process [34,39].

A linear correlation between $\ln(A)$ and E_a values was observed (Figure 8 (a)), what represents one of the various manifestations of the compensation effect. Unfortunately, these parameters are not independent, because they are derived from one and the same Arrhenius plot. Therefore, the kinetic compensation effect can be real when it is related to the isokinetic effect [33,39]. Thus, if true isokinetic temperature exists, the plots of $\ln(k)$ will all intersect at a common $1/T_{iso}$. Inspection of a series of plots shows wheth-

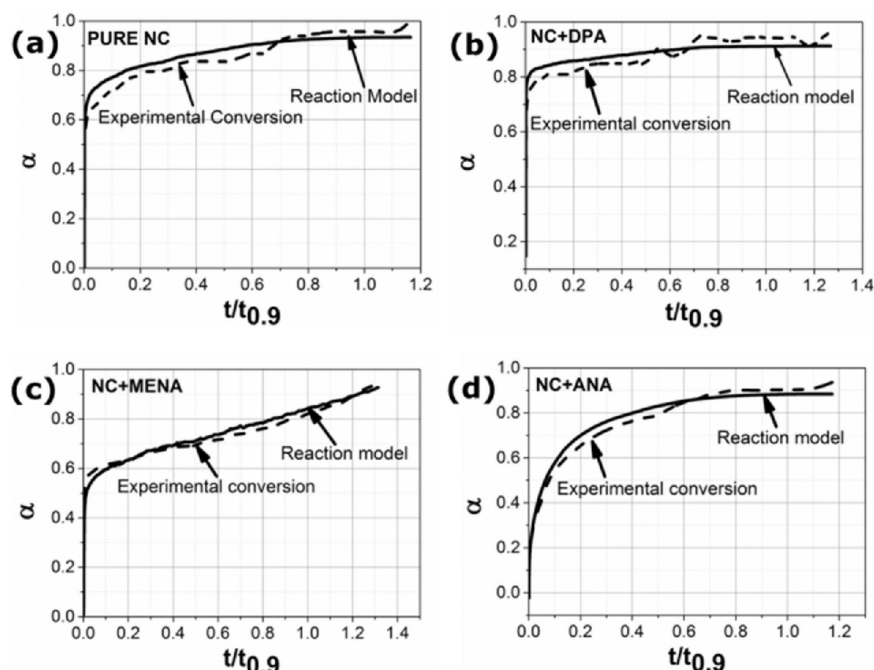


Figure 7. Reduced time plots for the reaction model and isothermal experimental data. The experimental data correspond to the average of three isothermal experiments performed at 90, 100, and 110 °C.

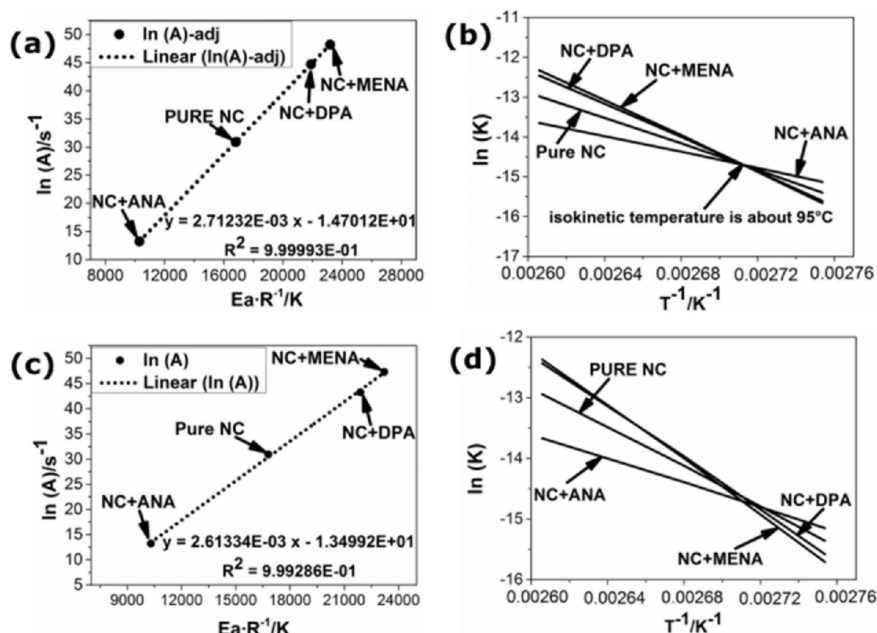


Figure 8. (a) Demonstration of the Kinetic compensation effect using the adjusted kinetic parameters; (b) Arrhenius lines for pure NC and its mixtures using the adjusted kinetic parameters; (c) Demonstration of the kinetic compensation effect using the original kinetic parameters; (d) Arrhenius lines for pure NC and its mixtures using the original kinetic parameters, indicating an isokinetic temperature.

er an $1/T_{\text{iso}}$ may exist. Initially, it is observed that two of the plots, using original kinetic parameters, fail to pass through the intersection (Figure 8 (c) and (d)). Based on the standard deviation of the computed $\ln(A)$ and E_a values, that

are constrained to intersect at postulated values $1/T$, the values of $\ln(A)$ and E_a are varied until a minimum deviation (Figure 8 (a)) is obtained in order to get a putative value for T_{iso} (95.5 °C). The adjusted values of $\ln(A)_{\text{adj}}$ and $E_{a\text{-adj}}$ are with-

in the determined standard deviations, what means that this isokinetic temperature is genuine. As shown in Figure 8 (b), a much increase of the decomposition rate of NC/ANA is found below against all others. In this sense, NC/ANA mixture is more reactive than other samples. This latter has a transition state at a much lower energy what is certainly caused by the compatibility issue.

4 Conclusions

The compatibility of nitrocellulose with several aniline-based compounds applied in gunpowder and solid propellants was investigated. The results showed that mixtures of NC/DPA and NC/MENA have good compatibilities as shown by DSC and VST. The other analytical techniques (FTIR, XRD, and densimetry) have provided additional valuable information for confirming the data derived from thermal techniques. However, chemical interactions have been found in the NC/ANA mixture based on thermal and non-thermal techniques. Furthermore, this work is concerned with the analysis of the apparent kinetic parameters and the isokinetic behavior to get information about the compatibility of some aniline-based organic compounds with nitrocellulose. The kinetic investigation is in accordance with the results obtained by other methods showing that ANA presents compatibility issues with nitrocellulose and consequently, can lead to similar problems when incorporated in propellant formulations. Finally, although the aniline-based compounds are considered as the best stabilizers for nitrate esters-based formulation, a compatibility investigation remains a key parameter to exploit fully their advantages.

References

- [1] W. P. C. de Klerk, N. van der Meer, R. Eerligh, Microcalorimetric study applied to the comparison of compatibility tests (VST and IST) of polymers and propellants, *Thermochim. Acta* **1995**, *269*, 231–243.
- [2] D. Trache, K. Khimeche, Study on the influence of ageing on chemical and mechanical properties of N, N'-dimethyl-N, N'-diphenylcarbamide stabilized propellants, *J. Therm. Anal. Calorim.* **2013**, *111*, 305–312.
- [3] J. P. Agrawal, *High energy materials: propellants, explosives and pyrotechnics*, John Wiley & Sons, Weinheim, Germany, **2010**.
- [4] M. Moniruzzaman, J. M. Bellerby, M. A. Bohn, Activation energies for the decomposition of nitrate ester groups at the anhydroglucopyranose ring positions C2, C3 and C6 of nitrocellulose using the nitration of a dye as probe, *Polym. Degrad. Stab.* **2014**, *102*, 49–58.
- [5] Q. Luo, T. Ren, H. Shen, J. Zhang, D. Liang, The Thermal Properties of Nitrocellulose: From Thermal Decomposition to Thermal Explosion, *Combust. Sci. Technol.* **2018**, *190*, 579–590.
- [6] D. Trache, K. Khimeche, A. Mezroua, M. Benziane, Physicochemical properties of microcrystalline nitrocellulose from Alfa grass fibres and its thermal stability, *Journal of Thermal Analysis and Calorimetry*. **2016**, *124*, 1485–1496.
- [7] D. Trache, K. Khimeche, Study on the influence of ageing on thermal decomposition of double-base propellants and prediction of their in-use time, *Fire Mater.* **2013**, *37*, 328–336.
- [8] W. P. C. de Klerk, Assessment of stability of propellants and safe lifetimes, Propellants, Explosives, *Pyrotechnics*. **2015**, *40*, 388–393.
- [9] M. Zayed, S. E. El-Begawy, H. E. Hassan, Mechanism study of stabilization of double-base propellants by using zeolite stabilizers (nano-and micro-clinoptilolite), *Arabian Journal of Chemistry*. **2017**, *10*, 573–581.
- [10] M. N. Boers, W. P. C. de Klerk, Lifetime prediction of EC, DPA, akardite II and MNA stabilized triple base propellants, comparison of heat generation rate and stabilizer consumption, Propellants, Explosives, *Pyrotechnics*. **2005**, *30*, 356–362.
- [11] M. Zayed, S. E. El-Begawy, H. E. Hassan, Enhancement of stabilizing properties of double-base propellants using nano-scale inorganic compounds, *J. Hazard. Mater.* **2012**, *227*, 274–279.
- [12] D. Trache, A. F. Tarchoun, Stabilizers for nitrate ester-based energetic materials and their mechanism of action: a state-of-the-art review, *J. Mater. Sci.* **2018**, *53*, 100–123.
- [13] D. Trache, A. F. Tarchoun, Analytical methods for stability assessment of nitrate esters-based propellants, *Crit. Rev. Anal. Chem.* **2019**, doi: 10.1080/10408347.2018.1540921.
- [14] Q. Tang, X. Fan, J. Li, F. Bi, X. Fu, L. Zhai, Experimental and theoretical studies on stability of new stabilizers for N-methyl-P-nitroaniline derivative in CMDB propellants, *J. Hazard. Mater.* **2017**, *327*, 187–196.
- [15] C. E. Lundell, O. T. O'Sullivan, M. R. Gau, M. J. Zdilla, Synthesis of Two Lead Complexes of Propellant Stabilizer Compounds: In Pursuit of Novel Propellant Additives, *ChemistrySelect*. **2017**, *2*, 11673–11676.
- [16] D. Trache, K. Khimeche, R. Benelmir, A. Dahmani, DSC measurement and prediction of phase diagrams for binary mixtures of energetic materials' stabilizers, *Thermochim. Acta* **2013**, *565*, 8–16.
- [17] D. Trache, K. Khimeche, M. Benziane, A. Dahmani, Solid-liquid phase equilibria for binary mixtures of propellant's stabilizers, *J. Therm. Anal. Calorim.* **2013**, *112*, 215–222.
- [18] D. Trache, K. Khimeche, A. Dahmani, Study of (solid-liquid) phase equilibria for mixtures of energetic material stabilizers and prediction for their subsequent performance, *Int. J. Thermophys.* **2013**, *34*, 226–239.
- [19] M. Abd-Elghany, A. Elbeih, S. Hassanein, Thermal behavior and decomposition kinetics of RDX and RDX/HTPB composition using various techniques and methods, *Cent. Eur. J. Energ. Mater.* **2016**, *13*, 714–735.
- [20] W. Pang, X. Fan, Y. Xue, H. Xu, W. Zhang, X. Zhang, Y. Li, Y. Li, X. Shi, Study on the compatibility of tetraethylammonium decahydrodecaborate (BHN) with some energetic components and inert materials, Propellants, Explosives, *Pyrotechnics*. **2013**, *38*, 278–285.
- [21] Q.-L. Yan, X.-J. Li, L.-Y. Zhang, J.-Z. Li, H.-L. Li, Z.-R. Liu, Compatibility study of trans-1, 4, 5, 8-tetranitro-1, 4, 5, 8-tetraazadecalin (TNAD) with some energetic components and inert materials, *J. Hazard. Mater.* **2008**, *160*, 529–534.
- [22] E. Krabbendam-La Haye, W. de Klerk, M. Miszczak, J. Szymanski, Compatibility testing of energetic materials at TNO-PML and MIAT, *J. Therm. Anal. Calorim.* **2003**, *72*, 931–942.
- [23] W. Guo, Z. Han, Q. Lin, B. Wang, Pre-formulation Compatibility Studies of 5-Amino-1H-tetrazole Nitrate with Several Typical Materials by Thermal and Non-thermal Techniques, *Cent. Eur. J. Energ. Mater.* **2018**, *15*, 100–114.

- [24] X. Li, Q.-H. Lin, X.-Y. Zhao, Z.-W. Han, B.-I. Wang, Compatibility of 2, 4, 6, 8, 10, 12-Hexanitrohexaazaisowurtzitane with a Selection of Insensitive Explosives, *J. Energ. Mater.* **2017**, *35*, 188–196.
- [25] A. Myburgh, Standardization on stanag test methods for ease of compatibility and thermal studies, *J. Therm. Anal. Calorim.* **2006**, *85*, 135–139.
- [26] A. Elbeih, M. Abd-Elghany, T. Elshenawy, Application of vacuum stability test to determine thermal decomposition kinetics of nitramines bonded by polyurethane matrix, *Acta Astronaut.* **2017**, *132*, 124–130.
- [27] G. Santhosh, H. G. Ang, Compatibility of Ammonium Dinitramide with Polymeric Binders Studied by Thermoanalytical Methods, *International Journal of Energetic Materials and Chemical Propulsion.* **2010**, *9*.
- [28] J. D. Gibson, Stabilizers for cross-linked composite modified double base propellants, in, *Google Patents*, **1995**.
- [29] R. Liu, W. Yu, T. Zhang, L. Yang, Z. Zhou, Nanoscale effect on thermal decomposition kinetics of organic particles: dynamic vacuum stability test of 1, 3, 5-triamino-2, 4, 6-trinitrobenzene, *Phys. Chem. Chem. Phys.* **2013**, *15*, 7889–7895.
- [30] D. Trache, F. Maggi, I. Palmucci, L. T. DeLuca, K. Khimeche, M. Fassina, S. Dossi, G. Colombo, Effect of amide-based compounds on the combustion characteristics of composite solid rocket propellants, *Arabian Journal of Chemistry.* **2015**, doi: 10.1016/j.arabjc.2015.11.016
- [31] D. Trache, Comments on “thermal degradation behavior of hypochlorite-oxidized starch nanocrystals under different oxidized levels”, *Carbohydr. Polym.* **2016**, *151*, 535–537.
- [32] D. Trache, A. Abdelaziz, B. Siouani, A simple and linear iso-conversional method to determine the pre-exponential factors and the mathematical reaction mechanism functions, *J. Therm. Anal. Calorim.* **2017**, *128*, 335–348.
- [33] M. B. Bushuev, D. P. Pishchur, E. B. Nikolaenkova, V. P. Krivopavlov, Compensation effects and relation between the activation energy of spin transition and the hysteresis loop width for an iron (II) complex, *Phys. Chem. Chem. Phys.* **2016**, *18*, 16690–16699.
- [34] N. Koga, A review of the mutual dependence of Arrhenius parameters evaluated by the thermoanalytical study of solid-state reactions: the kinetic compensation effect, *Thermochim. Acta.* **1994**, *244*, 1–20.
- [35] N. S. Agreement, 4147 (STANAG 4147), in, Chemical compatibility of ammunition components with explosives (non nuclear applications); AC/310 (SG1) D/15 (Draft edition 2) I-96 NAVY/ARMY/AIR.
- [36] A. Quye, D. Littlejohn, R. A. Pethrick, R. A. Stewart, Investigation of inherent degradation in cellulose nitrate museum artefacts, *Polym. Degrad. Stab.* **2011**, *96*, 1369–1376.
- [37] M. Hermann, Microstructure of nitrocellulose investigated by X-Ray diffraction, *42nd Int. Annual Conference of ICT*, Karlsruhe, Germany, June 28–July 1, **2011**, p. 53.
- [38] Y. Tong, R. Liu, T. Zhang, The effect of a detonation nanodiamond coating on the thermal decomposition properties of RDX explosives, *Phys. Chem. Chem. Phys.* **2014**, *16*, 17648–17657.
- [39] S. Vyazovkin, W. Linert, Thermally induced reactions of solids: Isokinetic relationships of non-isothermal systems, *Int. Rev. Phys. Chem.* **1995**, *14*, 355–369.

Manuscript received: September 3, 2018
Revised manuscript received: May 1, 2019
Version of record online: May 28, 2019